Turkish Journal of Electrical Engineering & Computer Sciences
http://journals.tubitak.gov.tr/elektrik/
Research Article
Turk J Elec Eng & Comp Sci
(2023) 31: 626 – 645

doi:10.55730/1300-0632.4006

An analytical solution of fractional order PI controller design for stable/unstable/integrating processes with time delay

Erdal ÇÖKMEZ[1], **İbrahim KAYA**[2,*]
Departments of Electrical and Electronics Engineering, Faculty of Engineering,
Dicle University, Diyarbakır, Türkey

Received: 05.10.2022 • **Accepted/Published Online:** 08.03.2023 • **Final Version:** 28.05.2023

Abstract: This paper aims to put forward an analytical solution for tuning parameters of a fractional order PI (FOPI) controller for stable, unstable, and integrating processes with time delay. Following this purpose, the analytical weighted geometrical center (AWGC) method has been extended to the design of fractional order PI controllers. To apply AWGC, the stability equations of the closed-loop system are written in terms of process and fractional order PI controller parameters. With the proposed method, the centroid can be calculated analytically, and the controller parameters can be easily calculated without the need of repetitive drawings of the stability boundary regions. Additionally, analytical equations are derived to calculate fractional integral order, λ, using the integral of squared error (ISE) objective function. The proposed analytical equations are simple and time-saving which might attract controller engineers for applying them on the industrial level. To show the efficiency of the suggested method compared to the given methods in the literature, several simulation examples are considered. Comparisons between the reported methods are figured out in terms of unit step responses for nominal and perturbed cases. Also, rise time, settling time, maximum sensitivity (Ms), integral of squared error (ISE), and total variation (TV) values are considered to compare the performance and robustness issues. Also, a real-time application of an inverted pendulum setup is deemed to prove the feasibility of the suggested method.

Key words: Fractional order PI controller, stability equations, weighted geometrical center, integrating process, unstable process, time delay

1. Introduction

The prevalence of PID controllers in industrial applications is an undoubted fact [1, 2]. Structural simplicity, availability to be designed with effective and simple methods, and performance robustness are the main advantages that enable PID controllers to be widely used in industrial applications [3, 4]. It was stated that 90% of the control loops used in industrial applications consist of PI/PID controllers [5, 6].

Fractional order PID controllers, defined as a general form of classical PID controllers, were proposed by Podlubny [7] after nearly 300 years of fractional calculus. Two new parameters, fractional integral and derivative provide flexibility in the tuning strategy of PID controllers [7] and better-shaped closed-loop responses to achieve more satisfactory results [5, 8]. Apart from that, the robustness can be increased with fractional orders [9, 10]. The mentioned advantages have attracted the attention of many scientists on fractional order PID controllers, and many studies have been introduced in the literature [5]. Furthermore, setting five parameters may also cause computational complexity [11]. To reduce that complexity, it is of great importance to improve the

*Correspondence: ikaya@dicle.edu.tr

performance of fractional order PI (FOPI) controllers. Hence, various methods have been proposed in the literature for this purpose. Monje et al. [12] suggested finding FOPI controller tuning parameters with the minimization of a nonlinear function for first and second-order stable plus time delay processes. The proposed method requires some user-defined parameters to calculate controller parameters. Chen et al. [13] proposed an F-MIGO-based FOPI controller design method, which needs recalculation of design steps when the process changes, for stable processes. Monje et al. [14] suggested the relay test based autotuning and nonlinear optimization via the MATLAB optimization toolbox for the design of fractional order controllers. In order to tune the controllers, frequency response parameters such as gain crossover frequency, phase margin, and the constraints on sensitivity function should be predefined. Gude and Kahoraho [15] designed a FOPI controller for stable processes with two new cost functions, one for low-frequency disturbance rejection and the other for control signal improvement. The proposed controller design method does not cover unstable first-order plus time delay (UFOPTD) and integrating first-order plus time delay (IFOPTD) processes. For stable first-order plus time delay processes, stability region based different design methods, for instance, implementable stability region [16] and gain-phase margin tester[17, 18] based design methods were porposed. In a study by Castillo-Garcia et al. [19], the robustness regions of the classical and fractional order PI controllers were compared for stable first-order plus time delay processes. The method, however, was suggested only for stable processes and does not provide an analytical answer for determining the value of the fractional integral order. Boudjehem and Boudjehem [20] used the integral of time absolute error (ITAE) value to minimize the error signal of the control system. Nonetheless, because the method lacks an analytical answer, changes in system parameters necessitate the repetition of optimization steps. Vu and Lee [21] introduced a FOPI controller design method based on Bode's ideal transfer function for stable first-order plus time delay processes. Despite their efforts to acquire an analytical answer, some design parameters in their design approach are still user-defined. They wanted to find controller settings that would allow for well-balanced set-point tracking and disturbance avoidance. Castillo-Garcia et al. [22] introduced a frequency domain stability analysis method which is called the region of feasible frequency specifications for stable first-order plus time delay processes. Although some analytical equations are derived, the provided equations must be used with user-defined parameters. The generalized Hermite-Biehler theorem was used by Hafsi et al. [11] to derive stability regions for stable first-order plus time delay systems. Stability regions were determined in terms of controller parameters, and adjusting parameters were chosen from those regions. However, no method or analytical equation for determining the suitable value of fractional integral order has been suggested. Using the approximated forms of FOPI controllers for stable first-order plus time delay processes, Rahimian and Tavazoei [23] suggested algebraic rules for the FOPI controllers. Although an analytical solution has been given, it is only applicable to open loop stable processes. Cases of UFOPT and IFOPTD are not addressed. In a study conducted by Yuce et al. [24], the ultimate frequency of the control system was obtained with the relay auto-tuning method, and the controller tuning parameters were calculated using the Ziegler-Nichols method for stable first-order plus time delay processes. Even so, the solution is not analytical and necessitates repeated drawings. Alagoz and Kaygusuz [25] proposed using a FOPI controller to manage the control of dynamic energy prices, and an implementation of automated energy balancing has been carried out in smart grid energy markets. However, no analytic solution has been suggested in their technique for tuning fractional integral order. Cokmez et al. [26] obtained stability regions of integrating first-order plus time delay processes under the control of the FOPI controller for specified gain and phase margins using the gain-phase margin tester. The method determines stability regions but does not include analytical methods for determining FOPI controller settings. Zhao et al. [8] suggested obtaining FOPI controller tuning parameters

with the extremum seeking algorithm, where the optimization was conducted for crossover frequency and phase margin, not directly for the FOPI controller tuning parameters. De Keyser et al. [27] proposed the fractional order KC autotuner-based FOPI controller design method for open-loop stable processes which needs a sine test and user-defined parameters. Later, Senol and Demiroglu [28] proposed a frequency domain based analytical design of FOPI controllers. In their method, to calculate controller tuning parameters, gain and phase-crossover frequencies should be selected. Therefore, the method needs user-defined parameters, too. Muresan et al. [29] proposed a disturbance attenuation based FOPI controller design method for various processes which needs repetitive drawings of RDR value and user-defined parameters. Ramadan et al. [30] proposed FOPI controller design based on metaheuristic optimization techniques such as harmony search (HS), modified flower pollination algorithm (MFPA), and electromagnetic field optimization (EFO). However, when process parameters change, the proposed method must rerun the optimization procedure.

The abovementioned literature review shows that analytical adjustment of FOPI controllers is extremely restricted. In general, the suggested methods allow users to manually select the fractional integral order. Furthermore, those that suggest analytical tuning necessitate the use of user-defined parameters or the recalculation of design stages when process parameters change. As a result, a solely analytical approach that does not require user-defined parameters or recalculation stages appears to be a gap in the design of the FOPI controller. Furthermore, FOPI controllers are typically intended for open-loop stable processes, with only a few uses for open-loop unstable/integrating processes. Based on the abovementioned literature analyses, the followings are the major contributions of this study:

- The AWGC method, which was used for integer order PI controllers and was shown to lead to somewhat robust performances [31], has been extended to the FOPI controllers.

- The AWGC approach was used to acquire fully analytical solutions for the design of the FOPI controllers that did not require any user-defined parameters or repeated sketches, as is typical in the literature. Because it is time-saving and straightforward, the proposed approach may be appealing for tuning controllers in industrial applications.

- Analytical tuning rules have been developed for identifying parameters of the FOPI controllers for controlling three different processes, namely SFOPTD, UFOPTD, and IFOPTD. To the best of the authors' knowledge, there are no studies in the literature that have taken into account all three process transfer functions mentioned above.

The effectiveness of derived tuning rules is investigated by conducting robustness analyses and performance results are compared in terms of rise time (tr), settling time (ts), integral of square error (ISE), total variation (TV), and maximum sensitivity (Ms). The paper continues as follows: In Section 2, a brief information is given about analytical weighted geometrical center (AWGC) method and the considered stable, unstable, and integrating processes. In Section 3, using the AWGC method, analytical equations are derived for FOPI controller tuning parameters. Next, robustness analyses have been carried out for stable, unstable, and integrating processes with different time delays in Section 4. In Section 5, simulation results, performance comparisons, and stability-robustness comparisons are given, and finally, conclusions are given in Section 6.

2. Preliminaries

2.1. Analytical weighted geometrical center (AWGC) method

The weighted geometrical center (WGC) method can be utilized to find the weighted geometrical center points (x_{WGC}, y_{WGC}) from the stability region. Due to using all points of the stability locus and the necessity of repeating the design stages as process transfer function changes, this method can be very time consuming [31]. With n defining the number of the sample points, and $f(x_k)$ and $g(x_k)$ are a set of real functions, the mathematical expressions for x_{WGC} and y_{WGC} points are, respectively, given by Onat et al. [32]:

$$x_{WGC} = \frac{1}{n}\sum_{k=1}^{n} f(x_k);\ f(x_1), f(x_2), ...f(x_k) \in \mathbb{R}. \tag{1}$$

$$y_{WGC} = \frac{1}{2n}\sum_{k=1}^{n} g(x_k);\ g(x_1), g(x_2), ...g(x_k) \in \mathbb{R}. \tag{2}$$

The analytical weighted geometrical center (AWGC) method [31] is the improved form of the WGC method. The AWGC method yields analytical equations in terms of the process and the controller parameters, hence the time-consuming disadvantages of the WGC method are eliminated [31]. Defining z as a continuous function in the [a,b] interval, the average value of z can be found as follows [31]:

$$z_{average} = \frac{1}{b-a}\int_a^b z(x)\,dx. \tag{3}$$

It is suggested to use following equations to analytically determine the centroid points of the stability region [31].

$$x_{AWGC} = \frac{1}{b-a}\int_a^b f(x)\,dx. \tag{4}$$

$$y_{AWGC} = \frac{1}{2(b-a)}\int_a^b g(x)\,dx. \tag{5}$$

2.2. Stable, unstable, and integrating processes

In this paper, FOPI controllers will be designed for stable first-order plus time delay (SFOPTD), unstable first-order plus time delay (UFOPTD), and integrating first-order plus time delay (IFOPTD) processes:

$$G(s) = \frac{Ke^{-\theta s}}{Ts+g} \quad \forall\ K>0\ \ \&\ \ \theta>0\ \ \&\ \ T>0\ \ \&\ \ g = \begin{cases} 1 & stable\ \ FOPTD \\ -1 & unstable\ \ FOPTD \end{cases} \tag{6}$$

$$G(s) = \frac{Ke^{-\theta s}}{s(Ts+1)}. \tag{7}$$

3. Fractional order PI controller design

The general form of the FOPI controller is given by

$$C(s) = K_p + \frac{K_i}{s^{\lambda}}. \tag{8}$$

where K_p, K_i, and λ represent proportional gain, integral gain, and fractional integral order, respectively. The control system is illustrated in Figure 1, where *C(s)* is the FOPI controller transfer function, and the $G_p(s)$ is the transfer function of the process.

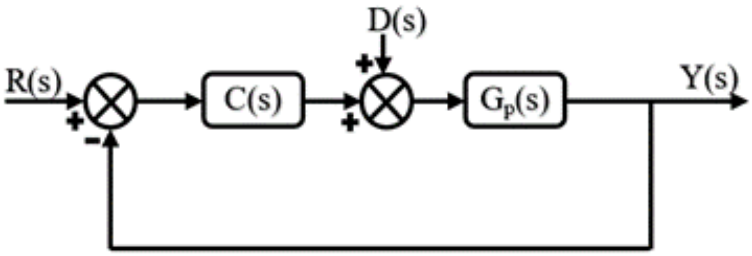

Figure 1. Closed-loop control system with unit feedback.

3.1. FOPI controller design for SFOPTD and UFOPTD processes

Assuming $g = 1$ in Equation (6) makes the system to be open-loop stable, while $g = -1$ turns the transfer function into an unstable one. In Equations (6) and (8), permorming $\tilde{s} = Ts$ the one obtains:

$$G_p(\tilde{s}) = \frac{Ke^{-}\tau\tilde{s}}{\tilde{s}+g}. \tag{9}$$

$$C(\tilde{s}) = K_p + \frac{K_i T^{\lambda}}{\tilde{s}^{\lambda}}. \tag{10}$$

where $\tau = \theta/T$. Thus, the characteristic equation of the control system given in Figure 1 is $1 + G_p(\tilde{s})C(\tilde{s}) = 0$. Substituting for $G_p(\tilde{s})$ and $C(\tilde{s})$ from Equations (9) and (10), respectively, one can obtain:

$$1 + \frac{Ke^{-\tau\tilde{s}}}{\tilde{s}+g}\frac{K_p\tilde{s}^{\lambda} + K_i T^{\lambda}}{\tilde{s}^{\lambda}} = 0. \tag{11}$$

Rearranging Equation (11) yields:

$$\Delta = \tilde{s}^{\lambda+1} + g\tilde{s}^{\lambda} + KK_p\tilde{s}^{\lambda}e^{-\tau s} + KK_i T^{\lambda}e^{-\tau s} = 0. \tag{12}$$

To find the stability region, three boundaries should be searched [8] using Equation (12):

- The real root boundary (RRB) is obtained by substituting $\tilde{s} = 0$ in (12), which results in $KK_i T^{\lambda} = 0$.
- The infinite root boundary (IRB) is obtained by replacing $\tilde{s} = \infty$ and equating the coefficient of the $\tilde{s}$ with the highest order to zero in (12). Since the coefficient of $\tilde{s}^{\lambda+1}$ can not be zero, IRB does not exist.
- The complex root boundary (CRB) is obtained by inserting $\tilde{s} = j\tilde{w}$ in Equation (12).

In order to find the CRB, $e^{-j\tau\tilde{w}} = \cos(\tau\tilde{w}) - j\sin(\tau\tilde{w})$, $j^2 = -1$ and $j^{\lambda} = \cos(\lambda\pi/2) + j\sin(\lambda\pi/2)$ definitions are used in Equation (12). Then, the real and imaginary parts of the equation are solved by equating to zero:

$$KK_p\tilde{w}^{\lambda}\cos(\lambda\pi/2 - \tau\tilde{w}) + KK_i T^{\lambda}\cos(\tau\tilde{w}) = \tilde{w}^{\lambda+1}\sin(\lambda\pi/2) - g\tilde{w}^{\lambda}\cos(\lambda\pi/2). \tag{13}$$

$$KK_p\tilde{w}^{\lambda}\sin(\lambda\pi/2-\tau\tilde{w})-KK_iT^{\lambda}\sin(\tau\tilde{w})=-\tilde{w}^{\lambda+1}\cos(\lambda\pi/2)-g\tilde{w}^{\lambda}\sin(\lambda\pi/2). \tag{14}$$

Solving Equations (13) and (14) for and yields the following expressions:

$$t(\tilde{w})=KK_p=(-\tilde{w}\cos(\lambda\pi/2+\tau\tilde{w})-g\sin(\lambda\pi/2+\tau\tilde{w}))/(\sin(\lambda\pi/2)). \tag{15}$$

$$f(\tilde{w})=KK_iT^{\lambda}=(-\tilde{w}^{\lambda+1}\cos(\tau\tilde{w})-g\tilde{w}^{\lambda}\sin(\tau\tilde{w}))/(\sin(\lambda\pi/2)). \tag{16}$$

To find an analytical solution of the centroid point of the stability region, Equations (15) and (16) are inserted into Equations (4) and (5), respectively. Defining $\cos(\lambda\pi/2+\tau w_c)=\alpha, \cos(\lambda\pi/2)=\beta, \sin(\lambda\pi/2+\tau w_c)=\sigma$ and $\sin(\lambda\pi/2)=\epsilon$ the analytical expressions obtained for $\mathrm{x_{AWGC}}$ and $\mathrm{y_{AWGC}}$ are found to be given by

$$x_{AWGC}=KK_p=\frac{1}{w_c}\int_0^{w_c}t(\tilde{w})\,d\tilde{w}=\frac{1}{w_c}\left[\frac{g(\alpha-\beta)}{\tau\epsilon}-\frac{\alpha+\tau w_c\sigma-\beta}{\tau^2\epsilon}\right]. \tag{17}$$

$$y_{AWGC}=KK_iT^{\lambda}=\frac{1}{2w_c}\int_0^{w_c}f(\tilde{w})\,d\tilde{w}=\frac{1}{2w_c\sin(\lambda\pi/2)}\int_0^{w_c}(-\tilde{w}^{\lambda+1}\cos(\tau\tilde{w})-g\tilde{w}^{\lambda}\sin(\tau\tilde{w}))\,d\tilde{w}. \tag{18}$$

Using the third order Taylor series approximations for $cos(\tau\tilde{w})$ and $sin(\tau\tilde{w})$, respectively, given by $\cos(\tau\tilde{w})=1-\frac{\tau^2\tilde{w}^2}{2!}+\frac{\tau^4\tilde{w}^4}{4!}$ and $\sin(\tau\tilde{w})=\tau\tilde{w}-\frac{\tau^3\tilde{w}^3}{3!}+\frac{\tau^5\tilde{w}^5}{5!}$, the analytical solution of $\mathrm{y_{AWGC}}$ obtained as follows:

$$y_{AWGC}=KK_iT^{\lambda}=\frac{1}{2w_c\sin(\lambda\pi/2)}\left[\frac{\left(g\tau^5+5\tau^4\right)w_c^{\lambda+6}}{120(\lambda+6)}-\frac{\left(g\tau^3+3\tau^2\right)w_c^{\lambda+4}}{6(\lambda+4)}+\frac{(g\tau+1)\,w_c^{\lambda+2}}{\lambda+2}\right]. \tag{19}$$

It is seen that Equations (17) and (19), which give analytical solutions of $\mathrm{x_{AWGC}}$ and $\mathrm{y_{AWGC}}$, depend on the value of w_c. Here, w_c is the critical frequency where the Nyquist plot of the process transfer function intersects the negative real axis. Since, the main purpose of this article is to obtain the FOPI controller parameters analytically, the critical frequency (w_c) must also be determined analytically. For this purpose, assuming $g=1$ for the SFOPTD process, and $g=-1$ for the UFOPTD process, the equation $f(\tilde{w})=0$ has been solved for τ varying in the range of [0.01, 10] for the SFOPTD process, and of [0.01, 0.99] for the UFOPTD process. It should be noted that the value of λ does not affect the value of the w_c. The obtained w_c values are shown in Figure 2 for different τ ranges and process transfer functions. Then, using a curve fitting tool, analytical expressions given in Equations (20) and (21) can easily be obtained. The obtained analytical expressions are also illustrated in Figure 2, which exhibit very good fittings. Consequently, for SFOPTD and UFOPTD processes the following expressions can be used to calculate the critical frequency value:

$$w_c=(-0.004415\tau^2+3.25\tau+4.17)/(\tau^2+2.654\tau+2.429e-06)\quad 0.01\le\tau\le 10\ \ \&\ \ g=1. \tag{20}$$

$$w_c=\frac{-4.423\tau^5+7.94\tau^4-5.249\tau^3+1.076\tau^2-0.7673\tau+1.575}{\tau+1.749e-05}\quad 0.01\le\tau\le 0.99\ \ \&\ \ g=-1. \tag{21}$$

It should be noted that for the UFOPTD process, the stability regions can be obtained only for $0.01\le\tau\le 0.99$.

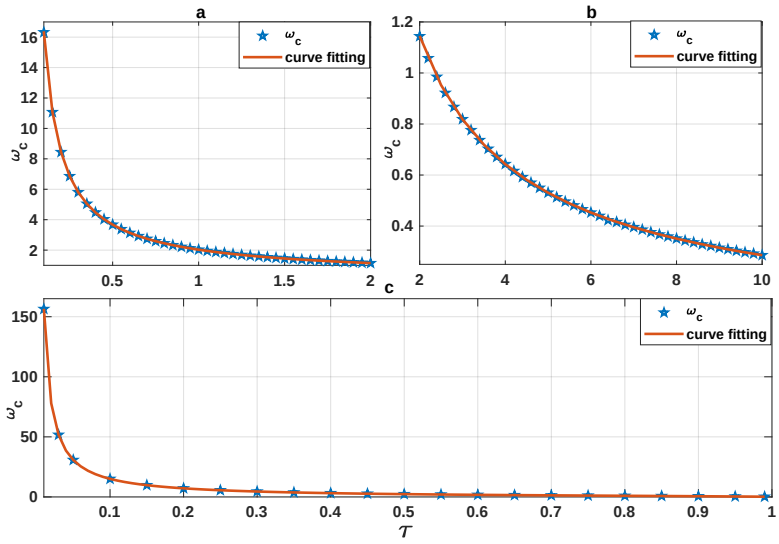

Figure 2. Curve fitting results to obtain critical frequency a) SFOPTD process, $0.01 \leq \tau \leq 2$; b) SFOPTD process, $2 \leq \tau \leq 10$; c) UFOPTD process, $0.01 \leq \tau \leq 0.99$.

Another important subject is the decision of fractional integral order, λ. In this study, ISE objective function is used to provide analytical formulae for the selection of an exact value of λ.

It is suitable to describe why ISE objective function was chosen to determine the value of λ at this point:

- It is common knowledge that using a PI/FOPI controller can result in significant initial errors due to an absence of a derivative component. On the other hand, it has been demonstrated that by using the ISE objective function, large errors can be punished more than smaller ones, and control systems that minimize ISE are available to rapidly eradicate large errors [33].
- When system dynamics deviations are taken into account, the ISE objective function has been shown to outperform other minimization functions [34].
- Furthermore, the efficacy of ISE-based fractional order controller design approaches has been demonstrated in a number of works [13, 35–38].

The mathematical formulation of ISE is given by $ISE = \int_0^\infty e^2(t)\,dt$ where $e(t)$ represents the error signal [39]. To obtain analytical formulae, the λ values were varied in the range of [0.1, 2] while normalized time delay, τ, varied in the range of [0.01, 10] for the SFOPTD and IFOPTD processes and [0.01, 0.99] for the UFOPTD process. The values that yield the lowest ISE value for each τ value were then found. The mathematical formulae for the choosing of λ in terms of τ values were then supplied using a curve fitting toolbox. The expression given in (22) has been provided for the selection of λ for the SFOPTD process. For $2 < \tau \leq 10$, there is a very small change in λ values, which provide the minimum ISE value. Therefore, an average value is provided for the λ value in this range.

$$\lambda = \begin{cases} (-0.03885\tau^3 + 1.385\tau^2 + 0.170\tau + 0.01997)/(\tau^2 + 0.2342\tau + 0.02449) & \& \;\; 0.01 \leq \tau \leq 2 \\ 1.240 & \& \;\; 2 < \tau \leq 10 \end{cases} \tag{22}$$

For the UFOPTD process case, τ has been varied in the range of [0.01, 0.99] and the λ value with the minimum ISE value has been calculated for each τ value. Then, using a curve fitting toolbox, the following expression has been obtained for the selection of λ for the UFOPTD process:

$$\lambda = 1.0651\exp(-6.8344\tau^{0.206}) - 1.545\tau^{1.495} + 2.312\tau + 0.01\tan(1.56\tau) + 0.721 \quad \& \quad 0.01 \leq \tau \leq 0.99. \tag{23}$$

Stability regions with centroid points are also provided for the SFOPTD and UFOPTD processes as seen in Figure 3. It has been observed that for both processes, increasing the value of τ causes smaller stability regions to be formed. It should be noted that stability regions have been obtained for $\lambda = 0.9$.

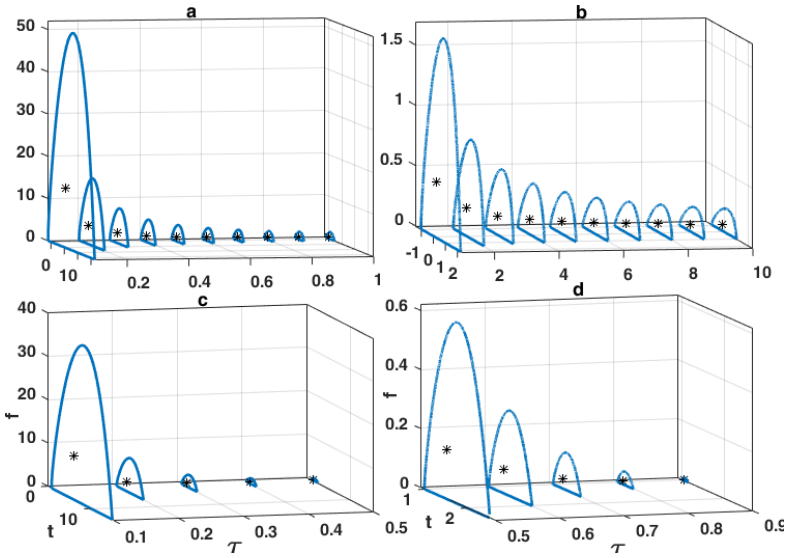

Figure 3. Stability regions a) SFOPTD process, $0.1 \leq \tau \leq 1$; b) SFOPTD process, $1 \leq \tau \leq 10$; c) UFOPTD process, $0.1 \leq \tau \leq 0.5$; d) UFOPTD process, $0.5 \leq \tau \leq 0.9$.

3.2. Fractional order PI controller design for IFOPTD process

The design steps for SFOPTD and UFOPTD processes in the previous section are followed in the same way for the IFOPTD process, given by Equation (7). Analytical equations for x_{AWGC} and y_{AWGC} have been obtained as given in Equations (24) and (25). The abbreviations used in the previous section apply here, as well.

$$x_{AWGC} = KK_pT = \frac{1}{w_c}\left[\frac{(2\alpha - 2\beta) - \tau^2(w_c^2\alpha + w_c\sigma) + \tau(2w_c\sigma + \beta - \alpha)}{\tau^3\epsilon}\right]. \tag{24}$$

$$y_{AWGC} = KK_iT^{\lambda+1} = \frac{1}{2w_c\sin(\lambda\pi/2)}\left[-\frac{\tau^5 w_c^{\lambda+8}}{120(\lambda+8)} + \frac{(4\tau^3+\tau^4)w_c^{\lambda+6}}{24(\lambda+6)} - \frac{(\tau^2+2\tau)w_c^{\lambda+4}}{2(\lambda+4)} + \frac{w_c^{\lambda+2}}{\lambda+2}\right]. \tag{25}$$

Similar to the previous section, the following expressions can be derived to analytically evaluate the critical frequency value for the IFOPTD process:

$$w_c = \begin{cases} \frac{0.0544\tau^4 - 0.2846\tau^3 + 0.6561\tau^2 + 0.5401\tau + 0.0165}{\tau^2 + 0.1396\tau + 0.0007045} & \& \quad 0.01 \leq \tau \leq 2 \\ \\ \frac{0.0001378\tau^3 - 0.003833\tau^2 + 0.04087\tau + 1.359}{\tau + 0.6495} & \& \quad 2 < \tau \leq 10. \end{cases} \tag{26}$$

For the IFOPTD process, following the concept given in subsection 3.1, the expression to calculate the value of λ for the minimum ISE value has been obtained as

$$\lambda = \begin{cases} (0.8169\tau^2 + 0.01674\tau + 0.0007827)/(\tau^2 + 0.0703\tau + 0.01828) & \& \;\; 0.01 \leq \tau \leq 2 \\ 0.79 & \& \;\; 2 < \tau \leq 5.5 \\ (0.02831\tau^3 + 0.124\tau^2 - 6.793\tau + 35.13)/(\tau^2 - 14.6\tau + 57.95) & \& \;\; 5.5 < \tau \leq 10 \end{cases} \tag{27}$$

Stability regions with centroid points are also provided for the IFOPTD process. Again, increasing values of τ, cause smaller stability regions as seen in Figure 4. Here the given stability regions are obtained for $\lambda = 0.9$.

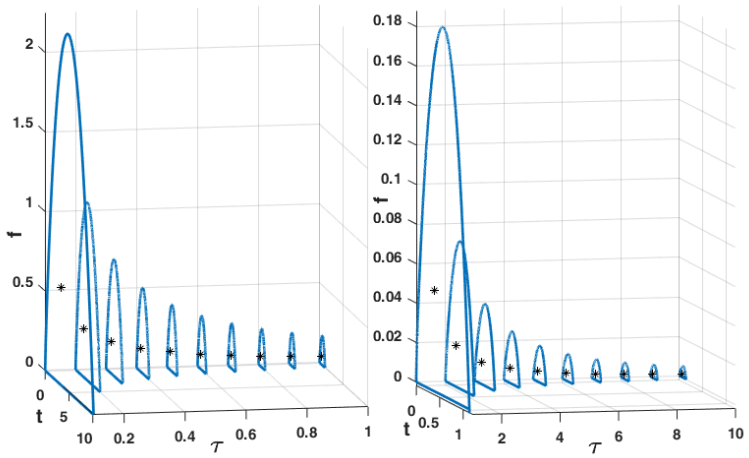

Figure 4. Stability regions of the IFOPTD process while $0.1 \leq \tau \leq 10$.

Finally, for the AWGC-based design of the FOPI controller, the procedure can be summarized as follows:

1. Obtain the normalized dead time ratio, $\tau = \theta/T$.
2. Use Equation (20) for the SFOPTD process, (26) for the UFOPTD process, and (28) for the IFOPTD process to find w_c value.
3. Evaluate the λ value using Equations (22),(23), and (27) for SFOPTD, UFOPTD, and IFOPTD processes, respectively.
4. Calculate x_{AWGC} and y_{AWGC} using Equations (17) and (19) for SFOPTD and UFOPTD processes (assume $g = 1$ for the SFOPTD, and $g = -1$ for the UFOPTD process), and (24)-(25) for the IFOPTD process.
5. Calculate the FOPI controller gain as $K_p = x_{AWGC}/K$ and $K_i = y_{AWGC}/KT^{\lambda}$ for the SFOPTD and UFOPTD processes, and $K_p = x_{AWGC}/KT$ and $K_i = y_{AWGC}/KT^{\lambda+1}$ for the IFOPTD process.

4. Robustness analysis

In this section, the robustness of the proposed FOPI controller is evaluated by considering the gain margin, phase margin, and maximum sensitivity (Ms) value. Ms is defined as the inverse of the shortest distance between the Nyquist plot of the process and the critical point $(-1 + j0)$. Typical values of the Ms [39] are desired to be in the range of [1.4, 2] for stable processes and greater than 2 for unstable processes. Smaller values of Ms result in sluggish responses but more robust performances. On the other hand, higher values of Ms yield faster

but less robust responses. Noting that the open loop transfer function of the system shown in Figure 1 is given by $L(jw) = C(jw)G_p(jw)$, then Ms can mathematically be calculated by

$$Ms = \max_{0 \le w < \infty} \left| \frac{1}{1 + L(jw)} \right|. \tag{28}$$

The other two well-known robustness measures are gain and phase margins which can be determined mathematically as: $GM = 1/(L(jw_p))$ and $PM = \pi + arg(L(jw_g))$. Here, w_p and w_g represent phase and gain crossover frequencies. Suggested values of gain and phase margins range in [2, 5] and $[30°, 60°]$ [31], respectively. The relation between Ms and gain-phase margins is $GM \ge Ms/(Ms-1)$ and $PM \ge 2\arcsin(1/(2Ms))$ [31].

For varying τ and λ values, robustness measures are obtained and listed in Tables 1–3 for SFOPTD, UFOPTD, and IFOPTD processes, respectively. Besides, unit step responses are shown in Figures 5, 7, and 9 for each considered process. For the SFOPTD process, as seen in Table 1, for $\tau = 0.5$ and $\tau = 1$, increasing the λ causes a slight increase in Ms value, while a noticeable decrease in gain and phase margins. On the other hand, for $\tau = 1.5$, increasing the λ provides a small decrease in Ms values and hence a more robust performance. Moreover smaller λ values may cause steady-state errors as seen in Figure 5.

Table 1. Robustness analysis for stable first-order plus time delay (SFOPTD) process.

τ	λ	K_p	K_i	GM	PM	Ms
0.5	0.8	0.6471	1.1072	3.2	59.56	1.66
	0.9	0.854	1.1103	3.09	57.38	1.66
	1	1.0507	1.2208	2.85	53.41	1.71
	1.1	1.2475	1.3342	2.65	50.99	1.76
	1.2	1.4544	1.4979	2.44	48.69	1.83
1	0.8	0.1506	0.5019	3.38	69.85	1.57
	0.9	0.3	0.49	3.42	64.83	1.57
	1	0.4421	0.4916	3.32	60.04	1.57
	1.1	0.5841	0.5064	3.11	55.36	1.58
	1.2	0.7335	0.5359	2.83	50.61	1.62
1.5	0.8	–0.0041	0.3407	3.16	72.23	1.59
	0.9	0.1273	0.3217	3.33	66.05	1.57
	1	0.2523	0.3122	3.44	60.44	1.56
	1.1	0.3773	0.311	3.36	54.77	1.55
	1.2	0.5087	0.3183	3.1	49.03	1.55

Apart from that, Ms values have been provided for varying τ and λ values as seen in Figure 6. As illustrated in the figure, the minimum Ms values can be obtained when τ varies in the range of [1, 2]. On the other hand, it is observed that λ values less than 0.5 and higher than 1.2 make the control system closer to instability. Consequently, λ values should be selected approximately in a range of [0.5, 1.2] for the SFOPTD process.

From Table 2, for the UFOPTD process, increasing the value of τ causes a deterioration in the robustness parameters. Higher τ values cause smaller gain-phase margins and higher Ms values. Also, it is observed that for $\tau = 0.25$ and $\tau = 0.5$, with smaller λ values, it is possible to increase the robustness, even if very small.

Table 2. Robustness analysis for unstable first-order plus time delay (UFOPTD) process.

τ	λ	K_p	K_i	GM	PM	Ms
0.25	0.8	2.5067	1.2094	1.94	20.6	3.04
	0.9	2.6703	1.3064	1.89	20.43	3.08
	1	2.8259	1.4499	1.83	20.25	3.13
	1.1	2.9814	1.6521	1.78	20.06	3.19
	1.2	3.145	1.9338	1.72	19.86	3.27
0.5	0.8	1.4863	0.1708	1.57	10.62	5.47
	0.9	1.5328	0.1692	1.54	10.61	5.49
	1	1.5769	0.1721	1.52	10.59	5.52
	1.1	1.6211	0.1798	1.5	10.55	5.56
	1.2	1.6675	0.1929	1.47	10.51	5.61
0.75	0.8	1.158	0.0236	1.25	3.54	16.22
	0.9	1.1694	0.0217	1.25	3.54	16.16
	1	1.1803	0.0206	1.24	3.55	16.14
	1.1	1.1912	0.02	1.24	3.56	16.11
	1.2	1.2027	0.0199	1.23	3.57	16.07

Table 3. Robustness analysis for integrating first-order plus time delay (IFOPTD) process.

τ	λ	K_p	K_i	GM	PM	Ms
0.5	0.8	0.6667	0.1232	2.44	26.63	2.65
	0.9	0.7199	0.1151	2.38	26.03	2.69
	1	0.7705	0.1106	2.32	25.48	2.75
	1.1	0.8211	0.109	2.27	24.93	2.81
	1.2	0.8743	0.1105	2.19	24.37	2.88
1	0.8	0.3556	0.057	2.44	30.53	2.37
	0.9	0.3901	0.0511	2.36	29.89	2.42
	1	0.4232	0.047	2.28	29.29	2.47
	1.1	0.4558	0.0445	2.2	28.71	2.53
	1.2	0.4904	0.0432	2.11	28.12	2.6
1.5	0.8	0.2501	0.0348	2.43	31.86	2.28
	0.9	0.2763	0.0304	2.34	31.23	2.33
	1	0.3012	0.0273	2.25	30.64	2.38
	1.1	0.3261	0.0251	2.16	30.07	2.44
	1.2	0.3523	0.0237	2.07	29.49	2.52

However, steady-state error that may occur in the system response, which is illustrated in Figure 7, should not be ignored. On the other hand, when $\tau = 0.75$, higher λ values provide very little improvement in system robustness. Additionally, as for the SFOPTD process, Ms values have been illustrated for varying τ values while $\lambda = 0.8, 0.9, 1, 1.1, 1.2$, and for varying λ values while $\tau = 0.25, 0.5, 0.75$ for the UFOPTD process as seen in Figure 8. From the figure, it is observed that higher τ values cause higher Ms values, thus less robustness.

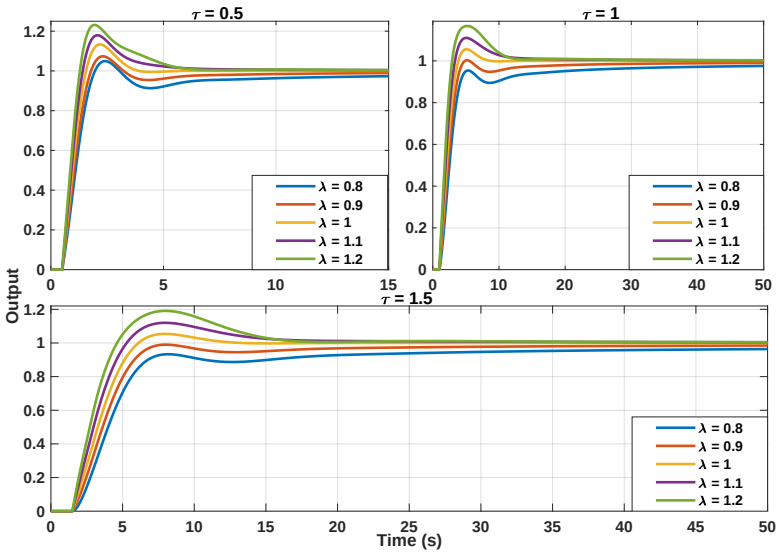

Figure 5. Unit step responses for the SFOPTD process for different τ values.

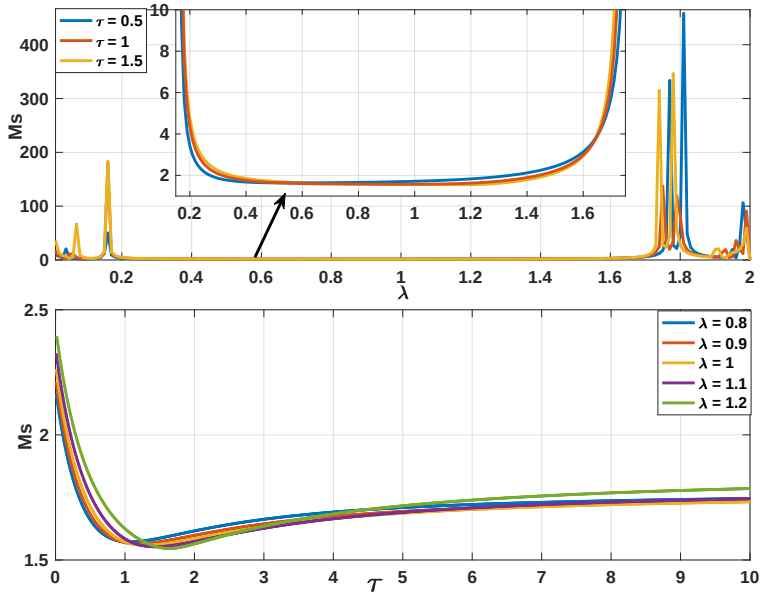

Figure 6. Ms values versus λ and τ for the SFOPTD process.

Moreover, λ values, which is less than 0.4 and higher than 1.5, are dangerous for the stability of the system.

The robustness measures of the IFOPTD process are given in Table 3, and the unit step responses are demonstrated in Figure 9. As can be seen from the table, for the IFOPTD process, an increase in λ value causes a higher Ms value, which refers to a less robust control system. Additionally, as seen in Figure 9, the smaller the value of λ, the improved system performance, albeit very small, in terms of the smaller overshoot.

As in the previous two cases, Ms values are provided for the IFOPTD process for varying λ and τ values, and the results are illustrated in Figure 10. Unlike the UFOPTD process, τ values less than 1 cause higher Ms values and consequently less robustness. But, for τ values higher than 1, smaller Ms values and more robust

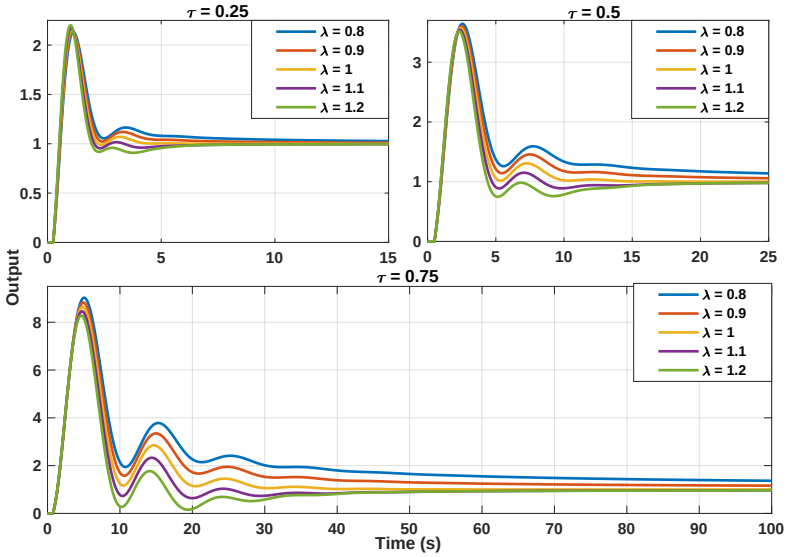

Figure 7. Unit step responses for the UFOPTD process for different τ values.

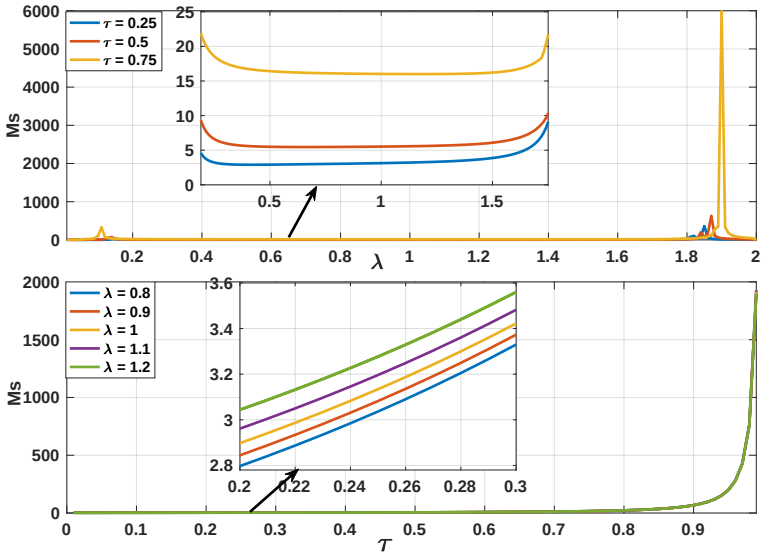

Figure 8. Ms values versus λ and τ values for the UFOPTD process.

systems can be obtained. Moreover, as seen in Figure 10, the λ value should be determined approximately in the range of [0.5, 1.2] to avoid instability.

5. Simulation results

In this section, several examples are considered to demonstrate the performance enhancement provided by the proposed AWGC based FOPI controller. The comparisons are given in terms of unit step responses, control signals, unit step responses with negative and positive perturbations in process parameters. While performing simulations, the FOMCON toolbox [40] has been utilized with an approximation order of N = 5 and a frequency range of [0.001, 1000]. Moreover, rise time, settling time, maximum sensitivity (Ms), ISE, and total variation

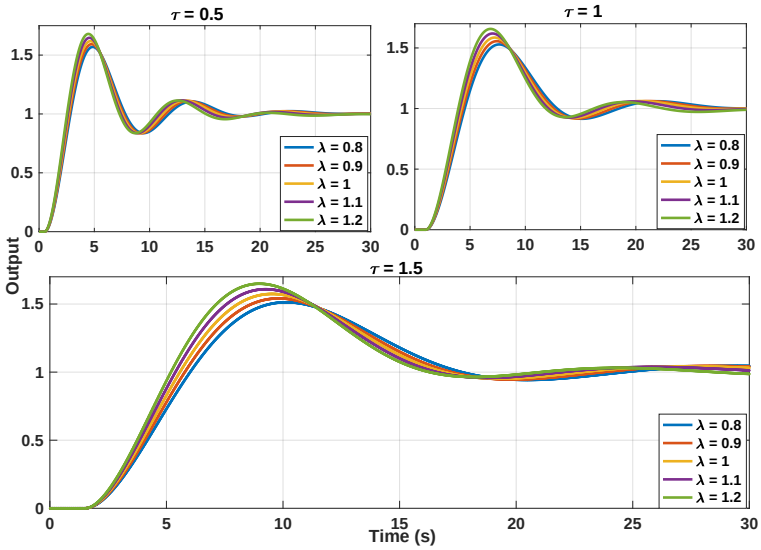

Figure 9. Unit step responses a for the IFOPTD process for different τ values.

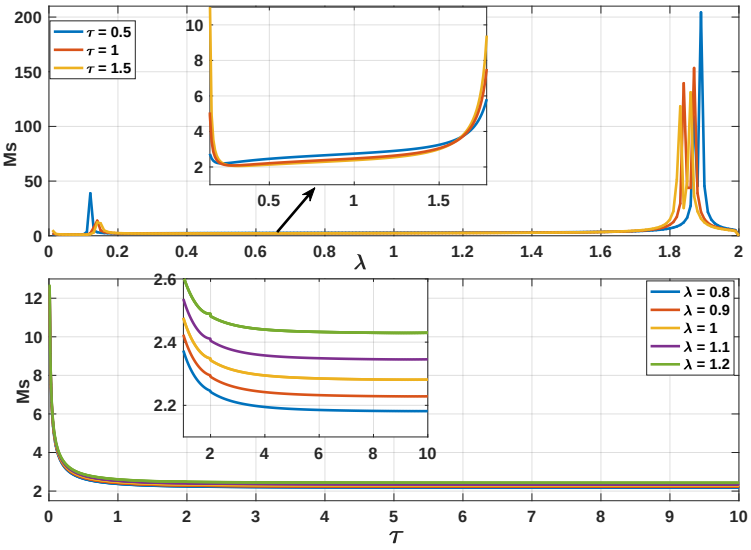

Figure 10. Ms values versus λ and τ values for the IFOPTD process.

(TV) values have been tabulated for the proposed method and the others used for comparison. TV value is an indication of the smoothness of the control signal and is defined as $TV = \sum_{i=0}^{\infty} |u_{i+1} - u_i|$. Here, u_i represents the input at the ith instant [39]. Smoother input results in a lesser TV value, while sharper input responses cause an increase in TV value.

Example 1: Stable first-order plus time delay (SFOPTD) process

Here, a process with transfer function of $G(s) = 0.55e^{-10s}/(62s + 1)$, which is previously considered by Monje et al. [12], is considered. They designed a FOPI controller having parameters of $K_p = 2.2326$, $K_i = 0.0285$ and $\lambda = 1.1274$. For the considered process, the methods proposed by Chen et al. [13] and Gude and Kahoraho

[15] give tuning parameters of $K_p = 3.89$, $K_i = 0.1428$, $\lambda = 0.9$ and $K_p = 3.845$, $K_i = 0.0603$, $\lambda = 1.1647$, respectively. The proposed FOPI controller has tuning parameters of $K_p = 6.2811$, $K_i = 0.2546$ and $\lambda = 0.943$.

The step responses are illustrated in Figure 11 for a unit step input and a disturbance input given in 500 s with a magnitude of 1. Additionally, performance indices are listed in Table 4. As seen in Figure 11 and Table 4, the proposed AWGC based FOPI controller gives better results in terms of settling time, rise time, and ISE values for both set point tracking and disturbance rejection. On the other hand, the other design methods have lesser TV values but longer settling times. Furthermore, the method proposed by Chen et al. [13] cannot reach the steady state position based on the 2% criterion. Additionally, the control signals for the considered design methods are illustrated in Figure 11, too. The proposed AWGC based FOPI controller has more initial control effort than the others, but faster settling times.

Table 4. Performance parameters for the SFOPTD process.

Method	$tr(s)$	$ts(s)$	Ms	ISE_s	ISE_{ld}	TV_s	TV_{ld}
Proposed FOPI	26.79	102.86	1.98	17.77	0.47	11.81	1.72
Monje et al. [12]	100.01	312.42	1.19	30.46	3.14	1.16	1.2
Chen et al. [13]	46.38	-	1.46	20.01	1.32	4.75	1.18
Gude and Kahoraho [15]	47.55	171.53	1.37	22.45	1.18	4	1.45

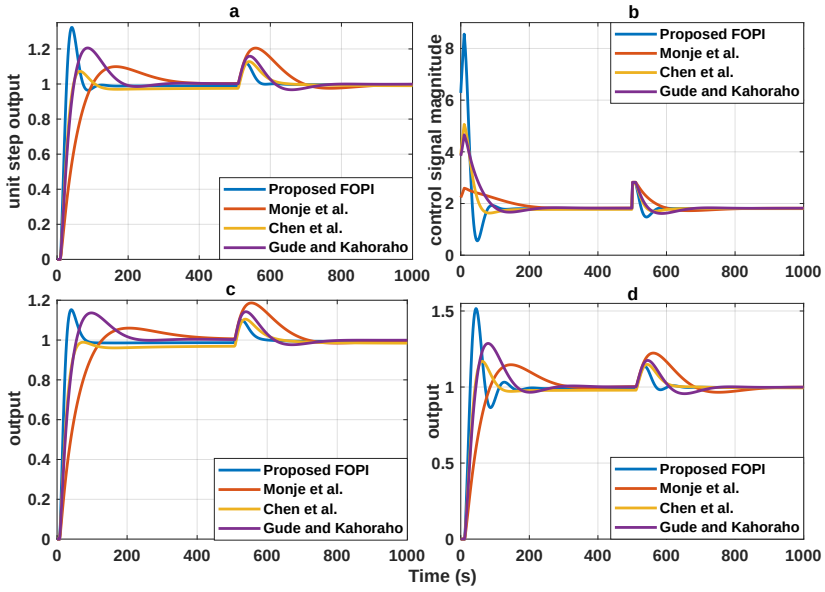

Figure 11. Performance results for the SFOPTD process. a) Unit step responses, b) control signals, c) negative perturbation of 20%, d) positive perturbation of 20% in the SFOPTD process parameters.

In case of parameter changes that may occur in the process, the designed controller should continue to control the process efficiently. The comparisons of the considered design methods under 20% negative and positive perturbation that may occur in process parameters, and are shown in Figure 11. In case of negative perturbation, the proposed FOPI controller continues to yield better unit step responses with shorter rise and settling times. Additionally, as seen from the figure, the disturbance rejection of the proposed method is better than the other design methods. On the other hand, the method proposed by Chen et al. [13] still cannot

deal with set point tracking. In the case of positive perturbation, the proposed FOPI controller has a slightly oscillatory response for set point tracking, but it is still better than the others for a faster settling time and disturbance rejection.

Example 2: Unstable first-order plus time delay (UFOPTD) process

A UFOPTD process, which was previously considered by Matausek and Sekara [41] is used to demonstrate the achieved performance enhancement with the proposed AWGC based FOPI controller. The transfer function of the considered UFOPTD process is $G(s) = 4e^{-2s}/(4s-1)$. For performance comparisons, the Matausek and Sekara [41] and the FOPI controller proposed by Muresan et al. [29] are used. The controller tuning parameters for the method proposed by Matausek and Sekara [41] are $K_p = 0.3381$, $K_i = 0.0028$, and the FOPI controller parameters for the method proposed by Muresan et al. [29] are $K_p = 0.3677$, $K_i = 0.0107$, and $\lambda = 1$. The proposed AWGC based FOPI controller has setting parameters of $K_p = 0.44$, $K_i = 0.0087$, and $\lambda = 1.34$.

The unit step responses of the UFOPTD process for the three design methods are illustrated in Figure 12 and the performance parameters are tabulated in Table 5. As seen from Figure 12 and Table 5, the proposed AWGC-based FOPI controller provides better performance for the UFOPTD process in terms of settling time, rise time, and integral of square error (ISE) for both set-point tracking and disturbance rejection. The method proposed by Muresan et al. [29] has smaller TV values but much longer settling times. Also, as seen from the figure, it is seen that the proposed FOPI controller has better control effort than the other compared methods.

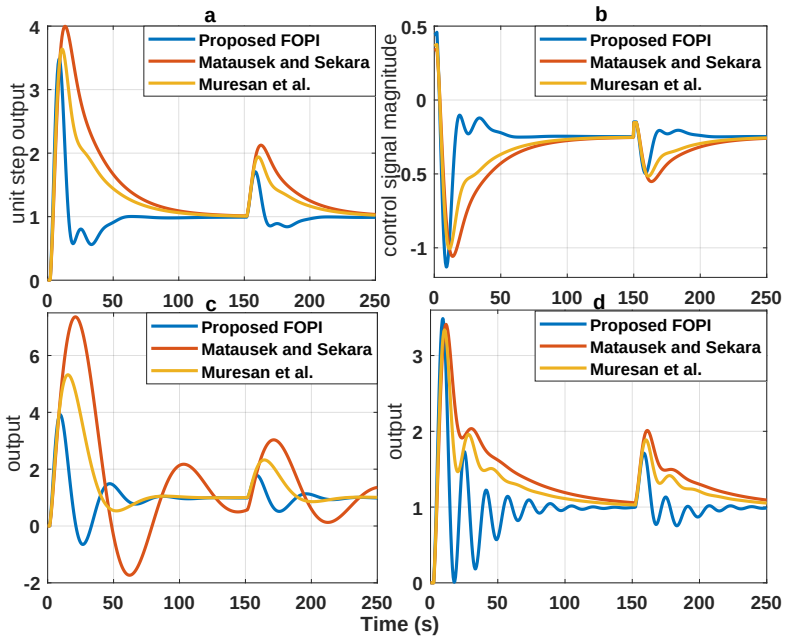

Figure 12. Performance results for the UFOPTD process. a) Unit step responses, b) control signals, c) negative perturbation of 20%, d) positive perturbation of 20% in the SFOPTD process parameters.

In the case of 20% perturbations occurring in process parameters, simulation results are shown in Figure 12. As seen from the figure, for both cases, the proposed FOPI controller has still better settling times compared to the method proposed by Matausek and Sekara [41] and the FOPI controller proposed by Muresan et al. [29].

Table 5. Performance parameters for the UFOPTD process.

Method	$tr(s)$	$ts(s)$	Ms	ISE_s	ISE_{ld}	TV_s	TV_{ld}
Proposed FOPI	3.78	56.6	5.73	63.85	3.459	3.008	3.1602
Matausek and Sekara [41]	4.20	138.31	4.07	186.2	23.01	2.215	3.1278
Muresan et al. [29]	4.06	128.94	4.17	117.9	12.51	2.149	3.0725

Example 3: Integrating first-order plus time delay (IFOPTD) process: inverted pendulum

In this section, the real time application on inverted pendulum has been carried out. The setup of the pendulum is shown in Figure 13. As seen in the figure, the cart is fixed with two pendulum arms and moves a 1-m track. The dc motor placed at the end of the rail is connected to the cart with the help of a belt. With the help of a dc motor and belt, the cart can be moved in two directions. The cart position and the pendulum angles are controlled with optical encoders. Due to the availability of modeling as an IFOPTD process, cart position control is only considered in this case. The transfer function of the cart position is [42]: G(s) = 0.64394/s(0.13605s+1). The time delay was considered 0.1 s in the process. In this case, the normalized time delay, τ, is 0.735. Using Equations (24), (25), and (27), the tuning parameters of the FOPI controller are: $K_p = 5.075$, $K_i = 4.3465$, and $\lambda = 0.745$. For comparison, the methods proposed by Shamsuzzoha and Skogestad [43], and Kos et al. [44] whose tuning parameters are: $K_p = 4.129$, $K_i = 2.271$ and $K_p = 3.289$, $K_i = 0.662$, respectively, are considered. Additionally, to deal with the overshoot, using the method proposed by Vijayan and Panda [45], set-point filters having transfer functions of $F(s) = 1/(0.758s+1)$, $F(s) = 1/(0.967s+1)$, and $F(s) = 1/(1.41s+1)$ have been designed for the proposed FOPI, the methods proposed by Shamsuzzoha and Skogestad [43], and Kos et al. [44], respectively. A step input having a magnitude of 0.25 m and a disturbance input having a magnitude of 0.1 at $t = 8s$ have been applied to the inverted pendulum system, and the step responses are displayed in Figure 13. It has been observed from the figure that, the proposed FOPI controller performed a satisfactory performance with less settling time and better disturbance rejection for the cart position control of the inverted pendulum.

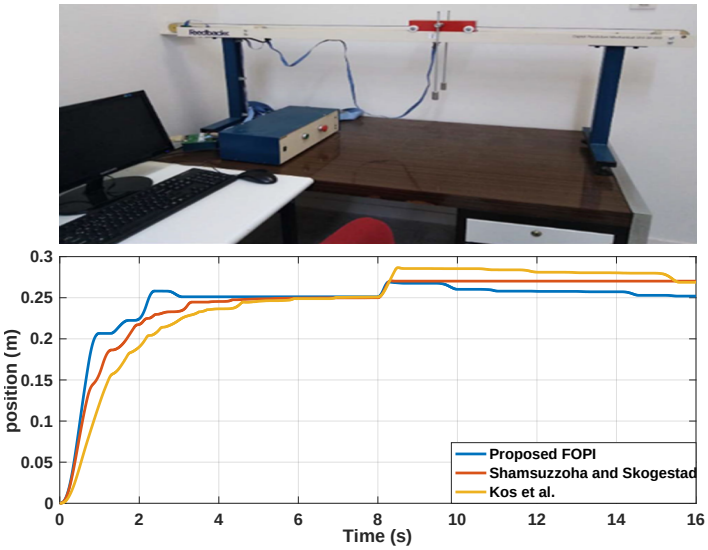

Figure 13. Experimental setup of the inverted pendulum and step responses.

6. Conclusion

The paper provided an analytical design of FOPI controllers for stable, unstable, and integrating processes with time delay. The previously proposed AWGC method for integer order PI controllers is extended to FOPI controllers, and the effectiveness of the introduced AWGC-based FOPI controller design method is demonstrated by simulation examples studied by others in the literature, as well as a real-time application of the inverted pendulum. Simulations were carried out in terms of unit step responses, disturbance rejection, process parameter changes, and the actuating signal that controls the process. Furthermore, the performance outcomes for set-point tracking and disturbance rejection were evaluated in terms of rise time, settling time, Ms value, ISE, and TV values. In addition to performance studies, robustness studies have been performed. The findings showed that by using the proposed design technique, it is feasible to improve the performance of a PI controller and obtain better closed-loop performances.

Nevertheless, the lack of the derivative part may cause significant initial errors and overshoots. To solve these issues, set-point filters are needed. As a result, set-point filters were used to deal with large overshoots in set-point tracking for the IFOPTD processes, as well as the real-time implementation of the inverted pendulum, which is also an integrating system.

In future work, we suggest using various controller structures, such as I-PD or PI-PD controllers, to improve the control system's efficiency and robustness. Besides that, improved performance outcomes can be achieved by employing modified Oustaloup approximation techniques.

References

[1] Åstrom KJ, Hagglund T. The future of PID control. Control Engineering Practice 2001; 9 (11): 1163–1175. doi: 10.1016/S0967-0661(01)00062-4

[2] Kasilingam G, Pasupuleti J. BBO algorithm-based tuning of PID controller for speed control of synchronous machine. Turkish Journal of Electrical Engineering & Computer Science 2016; 24 (4): 3274–3285.

[3] Saleem A, Soliman H, Al-Ratrout S, Mesbah M. Design of a fractional order PID controller with application to an induction motor drive. Turkish Journal of Electrical Engineering & Computer Science 2018; 26 (5): 2768–2778.

[4] Anwar MD, Pan S. A frequency response model matching method for PID controller design for processes with dead-time. ISA Transactions 2015; 55: 175-187. doi: https://doi.org/10.1016/j.isatra.2014.08.020

[5] Monje CA, Chen Y, Vinagre BM, Xue D, Feliu V. Fractional-Order Systems And Control Fundamentals And Applications. London: Springer-Verlag, 2010.

[6] De Keyser R, Muresan CI, Ionescu CM. A novel auto-tuning method for fractional order PI/PD controllers. ISA Transactions 2016; 62: 268-275. doi: https://doi.org/10.1016/j.isatra.2016.01.02

[7] Podlubny I. Fractional-Order Systems and PID-Controllers. IEEE Trans. Automat. Contr 1999; 44 (1): 208–214.

[8] Zhao J, Jing W, Wang J. An indirect optimization scheme for tuning a fractional order PI controller using extremum seeking. Mechatronics 2018; 56 : 146–156. doi: https://doi.org/10.1016/j.mechatronics.2018.11.003

[9] Rahimian MA, TavazoeiMS. Application of stability region centroids in robust PI stabilization of a class of second-order systems. Transactions of the Institute of Measurement and Control 2012; 34 (4): 487–498.

[10] Liu L, Zhang L, Pan G, Zhang S. Robust yaw control of autonomous underwater vehicle based on fractional-order PID controller. Ocean Engineering 2022; 257: doi: https://doi.org/10.1016/j.oceaneng.2022.111493.

[11] Hafsi S, Laabidi K, Farkh R. Synthesis of a fractional PI controller for a first-order time delay system. Transactions of the Institute of Measurement and Control 2013; 35 (8): 997–1007. doi: 10.1177/0142331212474018

[12] Monje CA, Calderon AJ, Vinagre BM, Chen Y, Feliu V. On Fractional PIλ Controllers: Some Tuning Rules for Robustness to Plant Uncertainties. Nonlinear Dynamics 2004; 38: 369–381.

[13] Chen Y, Bhaskaran T, Xue D. Practical Tuning Rule Development for Fractional Order Proportional and Integral Controllers. Journal of Computational and Nonlinear Dynamics 2008; 3 (2): 021403, 2008. doi: 10.1115/1.2833934

[14] Monje CA, Vinagre BM, Feliu V, Chen YQ. Tuning and auto-tuning of fractional order controllers for industry applications. Control Eng. Pract. 2008; 16 (7): 798–812. doi: https://doi.org/10.1016/j.conengprac.2007.08.006

[15] Gude JJ, Kahoraho E. Simple tuning rules for fractional PI controllers. In: 2009 IEEE Conference on Emerging Technologies & Factory Automation 2009; 1–8.

[16] Rahimian MA, Tavazoei MS. Stabilizing fractional-order PI and PD controllers: An integer-order implemented system approach. Journal of Systems and Control Engineering 2010; 224 (8): 893–903. doi: 10.1109/ETFA.2009.5347157

[17] Luo Y, Chen YQ. Stabilizing and robust fractional order PI controller synthesis for first order plus time delay systems. Automatica 2012; 48 (9): 2159-2167. doi: https://doi.org/10.1016/j.automatica.2012.05.072

[18] Sondhi S, Hote YV. Fractional-order PI controller with specific gain-phase margin for MABP control. IETE Journal of Research 2015;, 61 (2): 142–153. doi: 10.1080/03772063.2015.1009395

[19] Castillo-Garcia FJ, Feliu-Batlle V, Rivas-Perez R,Sanchez L. Comparative Analysis of Stability and Robustness between Integer and Fractional-Order PI Controllers for First Order plus Time Delay Plants. IFAC Proc. Vol. 2011; 44 (1): 15019–15024. doi: 10.3182/20110828-6-IT-1002.01875

[20] Boudjehem B, Boudjehem D. Parameter Tuning of a Fractional-Order PI Controller Using the ITAE Criteria. In: Fractional Dynamics and Control, New York: Springer, 2012, pp. 49–57.

[21] Vu TNL, Lee M. Analytical design of fractional-order proportional-integral controllers for time-delay processes. ISA Transactions 2013; 52 (5): 583–591. doi: https://doi.org/10.1016/j.isatra.2013.06.003

[22] Castillo-Garcia FJ, Feliu-Batlle V, Rivas-Perez R. Frequency specifications regions of fractional-order PI controllers for first order plus time delay processes. Journal of Process Control 2013; 23 (4): 598–612.

[23] Rahimian MA, Tavazoei MS. Improving integral square error performance with implementable fractional-order PI controllers. Optimal Control Application Methods 2014; 35: 303–323. doi: https://doi.org/10.1002/oca.2069

[24] Yüce A, Tan N, Atherton DP. Fractional Order PI Controller Design for Time Delay Systems. IFAC-PapersOnLine 2016; 49 (10): 94–99. doi: https://doi.org/10.1016/j.ifacol.2016.07.487

[25] Alagöz BB, Kaygusuz A. Dynamic energy pricing by closed-loop fractional-order PI control system and energy balancing in smart grid energy markets. Transactions of the Institute of Measurement and Control 2016; 38 (5): 565–578. doi: 10.1177/0142331215579949

[26] Çökmez E, Atiç S, Peker F, Kaya İ. Fractional-order PI Controller Design for Integrating Processes Based on Gain and Phase Margin Specifications. IFAC-PapersOnLine 2018; 51 (4): 751-756.

[27] De Keyser R, Muresan CI, Ionescu CM. Autotuning of a Robust Fractional Order PID Controller. IFAC-PapersOnLine 2018; 51 (25): 466–471. doi: https://doi.org/10.1016/j.ifacol.2018.11.181

[28] Şenol B, Demiroğlu U. Frequency frame approach on loop shaping of first order plus time delay systems using fractional order PI controller. ISA Transactions 2019; 86 : 192–200. doi: https://doi.org/10.1016/j.isatra.2018.10.021

[29] Muresan CI, Birs IR, Copot D, Dulf EH, Ionescu CM. Fractional-Order PI Controller Design Based on Reference – to – Disturbance Ratio. Fractal and Fractional 2022; 6 (4). doi: https://doi.org/10.3390/fractalfract6040224

[30] Ramadan HS, Padmanaban S, Mosaad MI. Metaheuristic-based near-optimal fractional order PI controller for on-grid fuel cell dynamic performance enhancement. Electric Power Systems Research 2022; 208: doi: https://doi.org/10.1016/j.epsr.2022.107897

[31] Alyoussef F, Kaya İ. Tuning proportional-integral controllers based on new analytical methods for finding centroid of stability locus for stable/unstable first-order plus dead-time processes. Proceedings of the Institution of Mechanical Engineers, Part I: Journal of Systems and Control Engineering 2021; 236 (4): 818-831.

[32] Onat C, Hamamci SE, Obuz S. A practical PI tuning approach for time delay systems. IFAC Proceedings Volumes 2012; 45 (14):102-107. doi: https://doi.org/10.3182/20120622-3-US-4021.00027

[33] Patel HR, Shah VA. Comparative study between Fractional Order PI D and Integer Order PID Controller: A case study of coupled conical tank system with actuator faults. 2019 4th Conference on Control and Fault Tolerant Systems (SysTol), Casablanca, Morocco, 2019; pp. 390-396, doi: 10.1109/SYSTOL.2019.8864772

[34] Farooq Z, Rahman A, Lone SA. Multi-stage Fractional-order Controller for Frequency Mitigation of EV-based Hybrid Power System. IETE Journal of Research. 2022; doi: https://doi.org/10.1080/03772063.2022.2061609

[35] Jesus IS, Tenreiro MJA. Fractional control of heat diffusion systems. Nonlinear Dynamics. 2008; 54: 263-282. doi: https://doi.org/10.1007/s11071-007-9322-2

[36] Sundaravadivu K, Arun B, Saravanan K. Design of Fractional Order PID controller for liquid level control of spherical tank. 2011 IEEE International Conference on Control System, Computing and Engineering, Penang, Malaysia, 2011: 291-295. doi: 10.1109/ICCSCE.2011.6190539

[37] Merrikh-Bayat F. General rules for optimal tuning the PI Dμ controllers with application to first-order plus time delay processes.The Canadian Journal of Chemical Engineering. 2012; 90 (6): 1400-1410. doi: https://doi.org/10.1002/cjce.21643

[38] Kesarkar AA, Selvaganesan N. Tuning of optimal fractional-order PID controller using an artificial bee colony algorithm. Systems Science Control Engineering. 2015; 3 (1): 99-105. doi:https://doi.org/10.1080/21642583.2014.987480

[39] Babu DC, Kumar DBS, Sree RP. Tuning of PID Controllers for Unstable Systems Using Direct Synthesis Method. Indian Chem. Eng. 2017; 59 (3): 215–241. doi: https://doi.org/10.1080/00194506.2016.1255570

[40] Tepljakov A, FOMCON: Fractional-Order Modeling and Control Toolbox. In: Fractional-order Modeling and Control of Dynamic Systems. Springer, Cham., 2017

[41] Mataušek MR, Šekara TB. PID controller frequency-domain tuning for stable, integrating and unstable processes, including dead-time. Journal of Process Control 2011; 21 (1): 17–27.

[42] Kaya İ, Peker F. Optimal I-PD controller design for setpoint tracking of integrating processes with time delay. IET Control Theory Appl. 2020; 14 (18): 2814–2824. doi: https://doi.org/10.1049/iet-cta.2019.1378

[43] Shamsuzzoha M, Skogestad S. The setpoint overshoot method: A simple and fast closed-loop approach for PID tuning. Journal of Process Control 2010; 20 (10): 1220–1234. doi:https://doi.org/10.1016/j.jprocont.2010.08.003

[44] Kos T, Huba M, Vrancic D. Parametric and Nonparametric PI Controller Tuning Method for Integrating Processes Based on Magnitude Optimum. Applied Sciences 2020; 10 (4):1443. doi:https://doi.org/10.3390/app10041443

[45] Vijayan V, Panda RC. Design of a simple setpoint filter for minimizing overshoot for low order processes. ISA Transactions 2012; 51 (2): 271–276. doi: https://doi.org/10.1016/j.isatra.2011.10.006